

Fine Microaneurysm Detection from Non-dilated Diabetic Retinopathy Retinal Images Using a Hybrid Approach

Akara Sopharak, Bunyarit Uyyanonvara and Sarah Barman

Abstract— Microaneurysms are the first clinical sign of diabetic retinopathy, a major cause of vision loss in diabetic patients. Early microaneurysm detection can help reduce the incidence of blindness. Automatic detection of microaneurysms is still an open problem due to their tiny sizes, low contrast and also similarity with blood vessels. It is particularly very difficult to detect fine microaneurysms, especially from non-dilated pupils and that is the goal of this paper. The process in this paper has two main segmentation steps. They are coarse segmentation using mathematic morphology and fine segmentation using naive Bayes classifier. A total of 18 microaneurysms features are proposed in this paper and they are extracted for naive Bayes classifier. The detected microaneurysms are validated by comparing at pixel level with ophthalmologists' hand-drawn ground-truth. The sensitivity, specificity, precision and accuracy were 85.68, 99.99, 83.34 and 99.99%, respectively.

Index Terms— diabetic retinopathy, microaneurysms, naive Bayes classifier.

I. INTRODUCTION

Diabetic retinopathy (DR) is the commonest cause of vision loss, and its prevalence is rising to 4.4% of the global population by 2030 [1]. In order to prevent the risk of blindness, diabetes patients need to have eye screening each year. It is time consuming and needs an expert on the screening process. However with a large number of patients, the number of ophthalmologists is not sufficient to cope with all patients, especially in rural areas or if the workload of local ophthalmologists is substantial. Therefore the automated computer system can help ophthalmologists to screen the patients more efficiently.

There are four stages used for grading DR, grade 0 (no DR), grade 1 (mild), grade 2 (moderate) and grade 3 (severe). Each grade is classified by an appearance and number of microaneurysms and haemorrhage. Microaneurysms (MA), are focal dilations of retinal

capillaries and appear as small round dark red dots. They appeared at the earliest clinically localized characteristic of DR, their detection would help to early treatment and prevent the blindness. It is difficult to detect MA because their pixels are similar to that of blood vessels. MA is hard to distinguish from noise or background variations because it has typically low contrast. In this paper we concentrate on MA detection as the earliest clinically localized characteristic of DR [2].

Previously published methods for MA detection have worked on fluorescein angiographies or color images taken on patients with dilated pupils in which the MA and other retinal features are clearly visible. The quality of non-dilated pupil retinal images will be worse and it greatly affects the performance of the mentioned algorithms.

The detection method proposed by T. Spencer et al. [3], M.J. Cree et al. [4] and A. Frame et al. [5] employ a mathematical morphology technique to segment MA within fluorescein angiograms. Gardner et al. [6] use a back propagation neural network on sub-images (20x20 or 30x30 pixel windows). C. Sinthanayothin et al. [7] propose an automated system of detection of diabetic retinopathy using recursive region growing segmentation (RRGS). D. Usher et al. [8] employ a combination of RRGS and adaptive intensity thresholding to detect candidate lesion regions and a neural network is used for classification. T. Walter et al. [9] propose a method based on diameter closing and kernel density estimation for automatic classification. B. Dupas et al. [10] use a diameter-closing to segment MA candidate regions and k-nearest neighbours (*k*NN) to classify MA. M. Niemeijer et al. [11] combine prior works by T. Spencer et al. [3] and A. Frame et al. [4] with a detection system based on pixel classification and new features are proposed. A *k*NN classifier was used in the final step. B. Zhang et al. [12] use multi-scale correlation coefficients (MSCF). They detect coarse MA candidate using MSCF and fine MA using features classification.

This paper has focused on automatic MA detection on images acquired without pupil dilation. A preliminary MA detection system is published using a set of optimally adjusted morphological operators [13]. In order to improve the performance of MA detection, fine segmentation enhancement using naive Bayes classifier is used.

II. METHOD

All digital retinal images taken from patients with non-dilated pupils were obtained from a KOWA-7

Manuscript received March 06, 2012; revised March 29, 2012.

A. Sopharak is with Faculty of Science and Arts, Burapha University, Chanthaburi Campus, 57 Moo 1, Kamong, Thamai, Chantaburi 22170, Thailand (phone: +66(0)39-310-000; e-mail: akara@buu.ac.th).

B. Uyyanonvara is with Sirindhorn International Institute of Technology, Thammasat University, 131 Moo 5, Tiwanont Road, Bangkokdi, Muang, Pathumthani, 12000, Thailand (e-mail: bunyarit@siit.tu.ac.th).

S. A. Barman is with Kingston University, Penrhyn Road, Kingston Upon Thames, Surrey, KT1 2EE, United Kingdom (e-mail: S.Barman@kingston.ac.uk).

non-mydratric retinal camera with a 45° field of view. The image size is 752 x 500 pixels with 24 bits per pixel.

The proposed system has three main steps. The preprocessing step includes noise removal, contrast enhancement and shade correction. Exudates and vessels are also detected and eliminated in this step. The second step, candidate MAs are detected by using a set of optimally adjusted mathematical morphology. And the last step, a fine MA detection is applied using the naive Bayes classifier in order to get an improvement in results.

The green plane (f_g) of the original image in RGB plane is used as red lesions such as MA and blood vessels have the highest contrast with the background in this color plane. A median filtering operation is applied on f_g to attenuate the noise before a Contrast Limited Adaptive Histogram Equalization was applied for contrast enhancement. A dark region (including noise and MAs) may dominate after contrast enhancement. To account for this, a shade correction algorithm is applied to the green band in order to remove slow background variation due to non-uniform illumination. A shade corrected image is accomplished by subtracting the image with a low pass filter, in this experiment, the result of a 35x35 median filter applied to the image to correct for background variation. Original green band image and shade corrected image are shown in Fig. 1 (a) and Fig. 1 (b), respectively.

We have to remove bright lesions such as exudates prior to the process because when they lie close together, small islands are formed between them and they can be wrongly detected as MAs. The morphological reconstruction method is used for exudate detection [14].

Vessels are another element in the image that needs to be removed prior the MA detection since MA and vessels both appear in a reddish color and MAs cannot occur on vessels. Candidate vessels are detected by the difference between the image after closing operator and the filled-in small black dot image. The objects on the difference image which have size smaller than 10 pixels (size of a MA) are then removed. The vessel and exudate detected results are shown in Fig. 2.

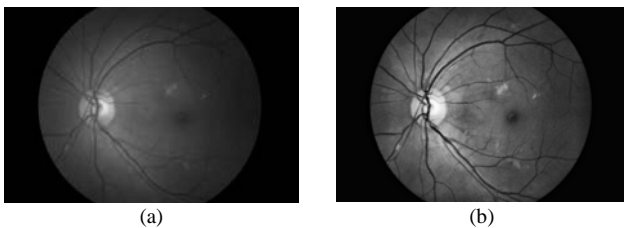


Fig. 1. Preprocessing steps. (a) Green band (b) Shade corrected image.

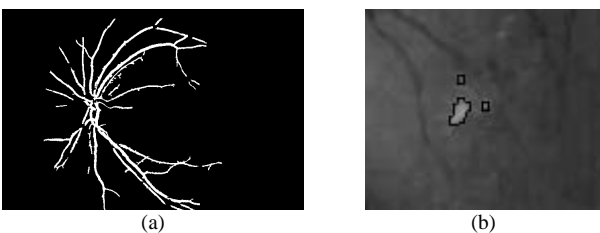


Fig. 2. Vessel and Exudate Detection. (a) Vessel detected (b) Exudate detected.

A. Coarse Segmentation using Mathematical Morphology

The main purpose for coarse segmentation is to identify MA candidates in a retinal image. Retinal MAs are focal dilations of retinal capillaries. They are discrete, localized saccular distensions of the weakened capillary walls and appear as small round dark red dots on the retinal surface. The diameter of a MA lies between 10 and 100 μm , but it always smaller than a diameter $\lambda < 125 \mu\text{m}$ [2], [3]. In our image set of size 752 x 500 pixels, the size of a MA is about 10 pixels.

A preprocessed retinal image is used as preliminary image for MA detection. The extended-minima transform is the regional minima of h-minima transform [23]. It is applied to the shade corrected image (f_{sc}) image. The output image f_E is a binary image with the white pixels represent the regional minima in the original image. The extended minima transform on the f_{sc} image with threshold value α_2 ($\alpha_2 = 0.05$ is used) is shown in (1).

$$f_E = EM(f_{sc}, \alpha_2) \quad (1)$$

where f_E is the output image.

The previous detected exudates and vessels were removed from the resulting image. The result is shown in Fig. 3(b).

$$f_{VE_removed} = f_E - f_{vesselT} - f_{ex} \quad (2)$$

where f_{ex} is the exudate detected image.

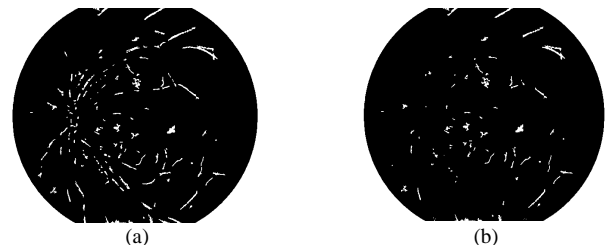


Fig. 3. Candidate Microaneurysm detection (a) Extended-minima transform image (b) Image after removal of vessels and exudates.

B. Feature Extraction

As an initial set of candidate per-pixel features, we propose 18 features potentially able to distinguish MA pixels from non-MA pixels:

- 1) The pixel's intensity value of shade corrected image (I_{sc}).
- 2) The pixel's intensity value of green band image after preprocessing (I_g).
- 3) The pixel's hue
- 4) The standard deviation of shade corrected image. A window size of 15x15 is used.
- 5) The standard deviation of green band image after preprocessing. A window size of 15x15 is used.
- 6) Six Difference of Gaussian (DoG) filter responses. The DoG filter subtracts one blurred version of an original image from another blurred version of the image [16]. We convolve with seven different Gaussian kernels with standard deviations of 0.5, 1, 2, 4, 8, 16, and 32. We use DoG1, DoG2, DoG3, DoG4, DoG5 and DoG6 to refer to the features

obtained by subtracting the image at scale $\sigma = 0.5$ from scale $\sigma = 1$, scale $\sigma = 1$ from $\sigma = 2$, scale $\sigma = 2$ from $\sigma = 4$, scale $\sigma = 4$ from $\sigma = 8$, scale $\sigma = 8$ from $\sigma = 16$, and scale $\sigma = 16$ from $\sigma = 32$, respectively.

- 7) *The area of the candidate MA.*
- 8) *The perimeter of the candidate MA.*
- 9) *The eccentricity of the candidate MA.*
- 10) *The circularity of the candidate MA.*
- 11) *The mean intensity of the candidate MA on shade corrected image.*
- 12) *The mean intensity of the candidate MA on green band image.*
- 13) *The ratio of the major axis length and minor length of the candidate MA.*

All 18 features are z-scale (transform to a mean of 0 and a standard deviation of 1) using the statistics of each feature over the training set.

C. Fine Segmentation using Naive Bayes Classifier

The result from the previous section is a rough estimation of the MA. In order to get a better result, a fine segmentation using naive Bayes classifier is applied in this step.

The naive Bayes classifier [15] - [17] uses the principle of Bayesian maximum a posteriori (MAP) classification: measure a finite set of features $\mathbf{x} = (x_1, \dots, x_n)$ then select the class

$$\hat{y} = \arg \max_y P(y|\mathbf{x})$$

where

$$P(y|\mathbf{x}) \propto P(\mathbf{x}|y)P(y) \quad (3)$$

$P(\mathbf{x}|y)$ is the likelihood of feature vector \mathbf{x} given class y , and $P(y)$ is the priori probability of class y . Naive Bayes assumes that the features are conditionally independent given the class:

$$P(\mathbf{x}|y) = \prod_i P(x_i|y)$$

We estimate the parameters $P(x_i|y)$ and $P(y)$ from training data.

After z-scaling, all of our features x_i are continuous, but the simple version of naive Bayes just described requires discrete features, so we perform unsupervised proportional k -interval discretization as implemented in Weka [18]. The technique uses equal-frequency binning, where the number of bins is the square root of the number of values.

III. RESULTS

Data sets of 45 non-dilated retinal images are performed preprocessing on an AMD Athlon 1.25 GHz PC using the MATLAB program. A set of 30 retinal images is used as a training set and 15 retinal images are used as a testing set. For each image in the training set, we computed the features for

every MA pixel then randomly selected and computed features from an equal number of non-MA pixels. The two sets of examples formed our training set. We thus obtained 4,546 samples, 2,273 examples of MA pixels and 2,273 examples of non-MA pixels, for training. From our test images, we used the 1,982 MA pixels and 5,638,018 non-MA pixels as a testing set. A Weka data mining software running on a standard PC for feature discretization and naive Bayesian classification is used.

Detected MAs are compared with the ophthalmologists' hand-drawn ground-truth images for verification. Sensitivity (Se), specificity (Sp), precision (Pr) and accuracy are chosen as measurement of the accuracy of the algorithms. All measures can be calculated based on four values, namely the true positive (TP) rate, the false positive (FP) rate, the false negative (FN) rate, and the true negative (TN) rate. These values are defined in Table I. From these quantities, the sensitivity is computed by $TP/TP+FN$, specificity is calculated by $TN/TN+FP$, precision is calculated by $TP/TP+FP$ and accuracy is calculated by $TP+TN/(TP+FN+TN+FP)$.

TABLE I
PIXEL BASED EVALUATION

Test Result	Disease Status	
	Present	Absent
Positive	True Positive (TP)	False Positive (FP)
Negative	False Negative (FN)	True Negative (TN)

Sensitivity, specificity, precision and accuracy in this experiment are 85.68, 99.99, 83.34 and 99.99%, respectively. The numbers of MAs are also counted for automated grading of the severity of the DR. A comparison of average result from mathematical morphology from our previous paper [13] and combined mathematical morphology with naive Bayes classifier is shown in Table II. Fig. 4 displays the comparison of MA detection from mathematical morphology, result of fine-tuned segmentation using naive Bayes classifier and ground truth image.

From our previous MA detection experiment using only mathematical morphology, there are some missing true MA pixels and some false MA detection on faint blood vessels appears. This experiment has shown that the proposed method could cope this problem. It could detect those misclassified MA (shown in yellow square box on Fig. 4 (c)) and reduces the false MA (shown in red circle on Fig.4 (c)).

TABLE II
COMPARISON OF AVERAGE RESULT FROM MATHEMATICAL MORPHOLOGY AND NAIVE BAYS CLASSIFIER

Method	Se(%)	Sp(%)	Pr(%)	Accuracy(%)
Morphology	81.61	99.99	63.76	99.98
Morphology+ Naive Bayes	85.68	99.99	83.34	99.99

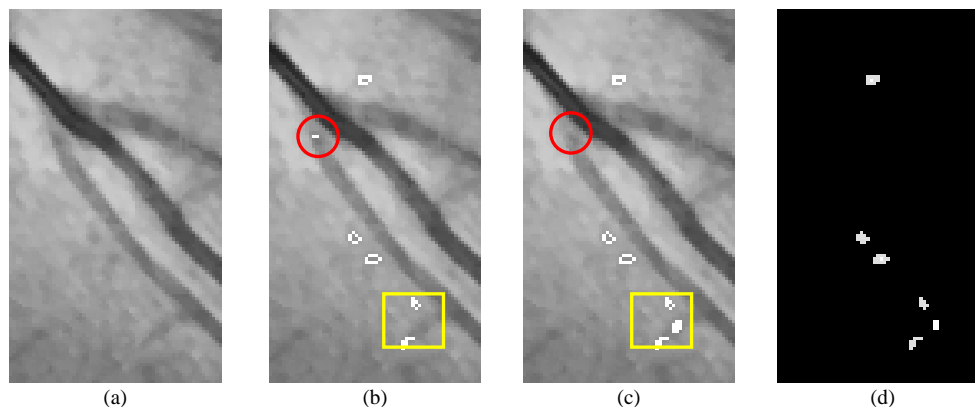


Fig. 4. Comparison of microaneurysm detection results. (a) Original image. (b) Result from morphology. (c) Result from naive Bayes classifier. (d) Ground truth image

VI. CONCLUSION AND DISCUSSION

In this paper we have investigated and proposed MA detection based on a hybrid approach of two segmentation techniques, namely, coarse segmentation using mathematical morphology and fine segmentation using naive Bayes classifier. The 18 per-pixel features are also proposed based on characteristic of MA. The results have shown that the sensitivity, precision and accuracy value increase after fine segmentation using naive Bayes classifier. The system also provided ophthalmologists with the number of MAs for the grading of the DR stage.

In future work, a data set should be expanded and the system should be clinically tested as a practical aid to help ophthalmologists screen patients for diabetic retinopathy symptoms quickly and easily. In addition, other techniques should be tested and compared to the system in order to get a better result.

ACKNOWLEDGMENT

This research is funded by the Burapha University, Chanthaburi Campus and National Research University Project of Thailand Office of Higher Education Commission (Thammasat University).

REFERENCES

- [1] S. Wild, G. Roglic, A. Green et al., "Global prevalence of diabetes: estimates for the year 2000 and projections for 2030," *Diabetes Care* 27, 2004, pp.1047-1053.
- [2] P. Massin, A. Erginay, and A. Gaudric, "Retinopathie Diabetique", Elsevier, Editions scientifiques de medicales, Elsevier, SAS, Paris 2000.
- [3] T. Spencer, J.A. Olson, K.C. McHardy et al., "An image-processing strategy for the segmentation and quantification of microaneurysms in fluorescein angiograms of the ocular fundus," *Comp Biomed Res* 29, 1996, pp. 284-302.
- [4] M.J. Cree, J.A. Olson, K.C. McHardy et al., "A fully automated comparative microaneurysm digital detection system," *Eye* 11, 1997, pp. 622-628.
- [5] A. Frame, P. Undrill, M. Cree et al., "A comparison of computer based classification methods applied to the detection of microaneurysms in ophthalmic fluorescein angiograms," *Comput. Biol. Med.* 28, 1998, pp. 225-238.
- [6] G. Gardner, D. Keating, T.H. Williamson et al., "Automatic detection of diabetic retinopathy using an artificial neural network: a screening tool," *Br J Ophthalmol* 80, 1996, pp.940-944.
- [7] C. Sinthanayothin, J.F. Boyce, T.H. Williamson, T.H. et al., "Automated Detection of Diabetic Retinopathy on Digital Fundus Image," *Diabetic Medicine* 19(2), 2002, pp. 105-112, 2002.
- [8] D. Usher, M. Dumskyj, M. Himaga et al., "Automated Detection of Diabetic Retinopathy in Digital Retinal Images: A Tool for Diabetic Retinopathy Screening," *Diabetic Medicine* 21(1), 2004, pp. 84-90.
- [9] T. Walter, P. Massin, A. Erginay et al., "Automatic detection of microaneurysms in color fundus images," *Medical Image Analysis* 11(6), 2007, pp.555-566.
- [10] B. Dupas, T. Walter, A. Erginay et al., "Evaluation of automated fundus photograph analysis algorithms for detecting microaneurysms, haemorrhages and exudates, and of a computer-assisted diagnostic system for grading diabetic retinopathy," *Diabetes & Metabolism* 36(3), 2010, pp. 213-220.
- [11] M. Niemeijer, B. van Ginneken, J. Staal et al., "Automatic detection of red lesions in digital color fundus photographs," *IEEE Trans Med Imaging* 24(5), 2005, pp.584-592.
- [12] B. Zhang, X. Wu, J. You et al., "Detection of microaneurysms using multi-scale correlation coefficients," *Pattern Recognition* 43(6), 2010, pp. 2237-2248.
- [13] A.Sopharak, B. Uyyanonvara, and S. Barman, Automatic Microaneurysm Detection from Non-dilated Diabetic Retinopathy Retinal Images Using Mathematical Morphological Methods. *IAENG International Journal of Computer Science* 38(3) (2011), 295-301.
- [14] A. Sopharak, B. Uyyanonvara, S. Barman et al., "Automatic detection of diabetic retinopathy exudates from non-dilated retinal images using mathematical morphology methods," *Computer Medical Imaging and Graphics* 32(8), 2008, pp. 720-727.
- [15] R.S. Kenneth, C.R. John, J. Matthew et al. (2006, June 15). Difference of Gaussians Edge Enhancement [Online]. Available: <http://micro.magnet.fsu.edu/primer/java/digitalimaging/processing/diffgaussians/index.html>
- [16] N. Friedman, D. Geiger, and M. Goldszmidt, "Bayesian network classifiers," *Machine Learning*. Vol. 29, pp.131-163, 1997.
- [17] O.D. Richard, E.H. Peter, and G.S. David, *Pattern Classification 2nd edition*, A Wiley-Interscience Publication, 2000, pp. 20-83.
- [18] X.Y. Wang, J. Garibaldi, and T. Ozen, "Application of The Fuzzy C-Means clustering Method on the Analysis of non Pre-processed FTIR Data for Cancer Diagnosis," *Internat. Conf. on Australian and New Zealand Intelligent Information Systems (ANZIIS)*, pp. 233-238, 2003.